

Temperature dependence of spin-polarized transport in ferromagnet/unconventional superconductor junctions

T. Hirai,^{1,2} Y. Tanaka,^{1,2} N. Yoshida,³ Y. Asano,⁴ J. Inoue,¹ and S. Kashiwaya^{2,5}

¹*Department of Applied Physics, Nagoya University, Nagoya, 464-8603, Japan*

²*CREST, Japan Science and Technology Corporation (JST), 464-8603, Japan*

³*Department of Microelectronics and Nanoscience, School of Physics and Engineering Physics, Chalmers University of Technology and Goteborg University, S-412 96 Goteborg, Sweden*

⁴*Department of Applied Physics, Hokkaido University, Sapporo 060-8628, Japan*

⁵*National Institute of Advanced Industrial Science and Technology, Tsukuba, 305-8568, Japan*

(Received 31 October 2002; published 1 May 2003)

Tunneling conductance in ferromagnet/unconventional superconductor junctions is studied theoretically as a function of temperature and spin polarization in ferromagnets. In d -wave superconductor junctions, a zero-energy Andreev bound state drastically affects the temperature dependence of the zero-bias conductance (ZBC). In p -wave superconductor junctions, numerical results show various temperature dependences of the ZBC depending on the direction of the magnetic moment in ferromagnets and the pairing symmetry in superconductors such as p_x -, p_y -, and $p_x + ip_y$ -wave symmetries. The last one is a candidate for the pairing symmetry of Sr_2RuO_4 . From these characteristic features in the conductance, we may obtain information about the degree of spin polarization in ferromagnets and the direction of the d vector in spin-triplet superconductors.

DOI: 10.1103/PhysRevB.67.174501

PACS number(s): 74.50.+r

I. INTRODUCTION

In recent years, transport properties in unconventional superconductor junctions have been studied both theoretically and experimentally. In these junctions, a zero energy state (ZES) (Refs. 1–3) formed at the junction interface plays an important role in the tunneling spectroscopy. It is now well known that the ZES is responsible for the zero-bias conductance peak (ZBCP) in the high- T_C superconductor junctions^{4–9} and related phenomena.^{10–21} The theoretical studies clearly relate the formation of the ZES to the ZBCP in tunneling spectroscopy.^{22–25} Since the formation of the ZES is a general phenomenon in unconventional superconductor junctions, the ZBCP is also expected in spin-triplet superconductor junctions.^{26–32} Actually, the ZBCP has been observed in junctions of Sr_2RuO_4 (Refs. 33,34) and UBe_{13} .³⁵ The ZBCP has also been theoretically predicted for organic superconductors $(\text{TMTSF})_2X$ very recently.^{36–38}

From the view of future device applications, transport properties in hybrid structures consisting of ferromagnets and superconductors have attracted much attention. It was pointed out that in ferromagnet/insulator/spin-singlet unconventional superconductor ($F/I/S$) junctions that the amplitude of the ZBCP decreases with increasing the magnitude of the exchange potential in ferromagnets. This is because the exchange potential breaks the time-reversal symmetry and suppresses the retroreflectivity of the Andreev reflection.^{39–46,49,50} Thus the ZBCP is sensitive to the degree of spin polarization in ferromagnets. Since the tunneling conductance is independent of the magnitude of the insulating barrier,⁵¹ it is possible to estimate the spin polarization in ferromagnets through the temperature dependence of the ZBCP. An experimental test could be carried out in $\text{La}_{0.7}\text{Sr}_{0.3}\text{MnO}_3/\text{YBa}_2\text{Cu}_3\text{O}_{7-x}$ junctions in the near future.^{52–55}

When spin-triplet superconductors are attached to ferromagnets,^{43,44} the ZBCP depends not only on the spin polarization but also on other parameters such as relative angles between the d vector in triplet superconductors and the magnetic moment in ferromagnets.^{31,32,45,46} Thus it may be possible to find details of the pair potential by comparing the characteristic feature of the ZBCP in theoretical calculations and those in experiments. For this purpose, it is necessary to know effects of other ingredients such as temperatures and the profile of the pair potential near the junction interface on the ZBCP. It is known that the amplitude of the pair potential is drastically suppressed at a surface or a interface of superconductors in the presence of the ZES.^{2,28,56–58,67} Although several studies on tunneling phenomena in ferromagnet/unconventional superconductor junctions have been made so far,^{47,48} such issues have never been addressed.

In this paper, we calculate the tunneling conductance in ferromagnet/unconventional superconductor junctions as a function of temperature and the degree of spin polarization in ferromagnets, where the spatial dependence of the pair potential is determined self-consistently based on the quasiclassical Green's function theory. We choose d -wave and $p_x + ip_y$ -wave symmetries for the pair potentials which are candidates for pairing symmetries of high- T_C cuprates and Sr_2RuO_4 , respectively. For comparison, we also study the conductance in p_x - and p_y -wave superconductor junctions. From the calculated results, we reach the following conclusions.

(1) In d -wave junctions with (110) orientation and p_x -wave junctions, an incident quasiparticle from a ferromagnet always feels the ZES irrespective of the incident angles. The zero-bias tunneling conductance (ZBC) at the zero temperature is insensitive to the barrier potential at the interface. This result indicates the possibility to estimate the

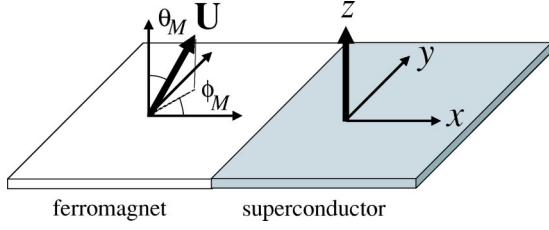


FIG. 1. Schematic illustration of a ferromagnet/superconductor junction. The direction of the magnetization axis is denoted by a polar coordinate (θ_M, ϕ_M) .

magnitude of the spin polarization of ferromagnets at sufficiently low temperatures (T) in experiments.

(2) In d -wave junctions with (110) orientation and p_x -wave junctions, the ZBC monotonically decreases with increasing temperatures for small magnitudes of spin polarization. On the other hand, for large magnitudes of polarization, the ZBC becomes an increasing function of temperature. While for d -wave junctions with (100) orientation and p_y -wave junctions, where the ZES does not appear, the ZBC is an increasing function of T independent of the spin polarization. For $p_x + ip_y$ -wave junctions, the ZBC first decreases with increasing T then increases.

(3) For p -wave junctions, the ZBC has various temperature dependences depending on the direction of the magnetic moment in ferromagnets. This unique property is peculiar to spin-triplet superconductors.

(4) Throughout this paper, we calculate the ZBC in two ways. (i) The spatial dependence of the pair potential is assumed to be the step function (non-SCF calculation). (ii) The spatial depletion of the pair potentials is determined self-consistently (SCF calculation). By comparing the conductance in these two ways, we found that the results in the non-SCF calculation are qualitatively the same as those in the SCF calculation.

The organization of this paper is as follows. In Sec. II, we formulate the tunneling conductance with an arbitrary angle between the magnetization axis of the ferromagnet and c axis of the superconductor. We show that the tunneling conductance depends on the direction of the magnetic moments only when superconductors have spin-triplet pairing. In Sec. III, we calculate the polarization and temperature dependence of ZBC for both d -wave and p -wave junctions. In Sec. IV, we summarize this paper.

II. FORMULATION

Let us consider a two-dimensional $F/I/S$ junction in the clean limit as shown in Fig. 1. We assume a flat interface at $x=0$. The insulator is described by the delta function $V(x) = H\delta(x)$, where H represents the strength of the barrier potential. We also assume that the Fermi energy E_F and the effective mass m in the ferromagnet are equal to those in the superconductor. The Stoner model is applied to describe ferromagnets, where the exchange potential U characterizes the ferromagnetism. The wave numbers in the ferromagnet for the majority (\uparrow) and the minority (\downarrow) spins are denoted by $k_{\uparrow(\downarrow)} = \sqrt{(2m/\hbar^2)[E_F + (-)U]}$. The wave functions $\Psi(\mathbf{r})$

are obtained by solving the Bogoliubov–de Gennes (BdG) equation under the quasiclassical approximation^{59,60}

$$E\Psi(\mathbf{r}) = \int d\mathbf{r}' \tilde{H}(\mathbf{r}, \mathbf{r}') \Psi(\mathbf{r}'), \Psi(\mathbf{r}) = \begin{pmatrix} u_{\uparrow}(\mathbf{r}) \\ u_{\downarrow}(\mathbf{r}) \\ v_{\uparrow}(\mathbf{r}) \\ v_{\downarrow}(\mathbf{r}) \end{pmatrix}, \quad (1)$$

$$\tilde{H}(\mathbf{r}, \mathbf{r}') = \begin{pmatrix} \hat{H}(\mathbf{r})\delta(\mathbf{r}-\mathbf{r}') & \hat{\Delta}(\mathbf{r}, \mathbf{r}') \\ \hat{\Delta}^\dagger(\mathbf{r}, \mathbf{r}') & -\hat{H}^*(\mathbf{r})\delta(\mathbf{r}-\mathbf{r}') \end{pmatrix},$$

where E is the energy of a quasiparticle measured from E_F , $\hat{H}(\mathbf{r}) = h_0 \hat{\mathbf{1}} - \mathbf{U}(\mathbf{r}) \cdot \boldsymbol{\sigma}(\mathbf{r})$, $h_0 = -(\hbar^2/2m)\nabla^2 + V(x) - E_F$, $\mathbf{U}(\mathbf{r}) = U\Theta(-x)\mathbf{n}$, and $\hat{\mathbf{1}}$ and $\boldsymbol{\sigma}$ are the 2×2 identity matrix and the Pauli matrix, respectively. Here \mathbf{n} points the direction of the magnetic moment in ferromagnets and $\Theta(x)$ is the Heaviside step function. The indices \uparrow and \downarrow denote the spin degree of freedom of a quasiparticle in superconductors. The magnetization axis in ferromagnets is represented in a polar coordinate (θ_M, ϕ_M) as shown in Fig. 1. We assume that the quantization axis of spin in the triplet superconductors is in the c axis which is parallel to the z direction. At first, we assume that the pair potential is a constant independent of x ,

$$\hat{\Delta}(\theta_S, x) = \hat{\Delta}(\theta_S)\Theta(x), \quad (2)$$

where $\hat{\Delta}(\theta_S)$ does not have the spatial dependence and $k_x = k_F \cos \theta_S$ and $k_y = k_F \sin \theta_S$ are the wave number in superconductors with k_F being the Fermi wave number. The pair potential $\hat{\Delta}(\theta_S)$ is given by

$$\hat{\Delta}(\theta_S) = \begin{pmatrix} \Delta_{\uparrow\uparrow}(\theta_S) & \Delta_{\uparrow\downarrow}(\theta_S) \\ \Delta_{\downarrow\uparrow}(\theta_S) & \Delta_{\downarrow\downarrow}(\theta_S) \end{pmatrix}. \quad (3)$$

The Hamiltonian in Eq. (2) is written in the coordinate of the spin space in the superconductor. It is comprehensive to rewrite the Hamiltonian in the coordinate of spin space in the ferromagnet since this notation is useful for considering scattering processes. The Hamiltonian in the coordinate of spin space in the ferromagnet is obtained by using the following unitary transformation:

$$\tilde{H}_F(\mathbf{r}, \mathbf{r}') = \tilde{U}^\dagger \tilde{H}(\mathbf{r}, \mathbf{r}') \tilde{U}, \quad (4)$$

$$\tilde{U} = \begin{pmatrix} \hat{U} & 0 \\ 0 & \hat{U}^* \end{pmatrix}, \quad \hat{U} = \begin{pmatrix} \gamma_1 & -\gamma_2^* \\ \gamma_2 & \gamma_1^* \end{pmatrix}, \quad (5)$$

$$\gamma_1 = \cos \frac{\theta_M}{2} e^{-i\phi_M}, \quad \gamma_2 = \sin \frac{\theta_M}{2} e^{i\phi_M}, \quad (6)$$

where \hat{U} is the operator which diagonalizes the $\hat{H}(\mathbf{r})$. The effective pair potential in the coordinate of spin space in the ferromagnet is rewritten as

$$\hat{\Delta}^F(\theta_S) = \hat{U}^\dagger \hat{\Delta}(\theta_S) \hat{U}^*. \quad (7)$$

Here, we consider the four types of pair potentials d -, p_x -, p_y -, and $p_x + ip_y$ -wave symmetries in superconductors. In the d -wave case, the pair potential is described as

$$\Delta_{\uparrow\downarrow}(\theta_S) = -\Delta_{\downarrow\uparrow}(\theta_S) \equiv \Delta_0 f(\theta_S), \quad (8)$$

$$\Delta_{\uparrow\uparrow}(\theta_S) = \Delta_{\downarrow\downarrow}(\theta_S) = 0, \quad (9)$$

$$f(\theta_S) = \cos[2(\theta_S - \alpha)], \quad (10)$$

where α is the angle between the a axis of the high- T_c superconductors and the interface normal. The effective pair potential in the coordinate of spin space in the ferromagnet is given by

$$\hat{\Delta}^F(\theta_S) \equiv \begin{pmatrix} \Delta_{\uparrow\uparrow}^F(\theta_S) & \Delta_{\uparrow\downarrow}^F(\theta_S) \\ \Delta_{\downarrow\uparrow}^F(\theta_S) & \Delta_{\downarrow\downarrow}^F(\theta_S) \end{pmatrix}, \quad (11)$$

$$= \begin{pmatrix} 0 & \Delta_0 f(\theta_S) \\ -\Delta_0 f(\theta_S) & 0 \end{pmatrix}, \quad (12)$$

$$= \hat{\Delta}(\theta_S). \quad (13)$$

As shown in Eq. (13), the expression of the pair potential remains unchanged under the transformation in Eq. (4). Therefore transport properties are expected to be independent of the direction of the magnetic moment. This conclusion can be applied to any spin-singlet superconductors. On the other hand, in spin-triplet superconductors, the pair potentials are given by

$$\Delta_{\uparrow\downarrow}(\theta_S) = \Delta_{\downarrow\uparrow}(\theta_S) = \Delta_0 f(\theta_S), \quad (14)$$

$$\Delta_{\uparrow\uparrow}(\theta_S) = \Delta_{\downarrow\downarrow}(\theta_S) = 0, \quad (15)$$

where the direction of the d vector is parallel to the c axis and

$$f(\theta_S) = \begin{cases} \cos \theta_S & \text{for } p_x \text{ symmetry,} \\ \sin \theta_S & \text{for } p_y \text{ symmetry,} \\ e^{i\theta_S} & \text{for } p_x + ip_y \text{ symmetry.} \end{cases} \quad (16)$$

Because the spin degree of freedom of Cooper pairs is active in triplet superconductors, the pair potential after the transformation in Eq. (4) depends on the direction of the magnetic moment

$$\hat{\Delta}^F(\theta_S) = \begin{pmatrix} \sin \theta_M & \cos \theta_M \\ \cos \theta_M & -\sin \theta_M \end{pmatrix} f(\theta_S) \Delta_0. \quad (17)$$

There are four reflection processes when an electron with the majority spin is incident from ferromagnets: (i) Andreev reflection to majority spin ($a_{\uparrow\uparrow}$), (ii) Andreev reflection to minority spin ($a_{\uparrow\downarrow}$), (iii) normal reflection to majority spin ($b_{\uparrow\uparrow}$), and (iv) normal reflection to minority spin ($b_{\uparrow\downarrow}$). Similar reflection processes are also possible, when an electron with the minority spin is incident from ferromagnets. The Andreev and normal reflection coefficients are denoted

by $a_{\bar{s}\bar{s}'}$ and $b_{\bar{s}\bar{s}'}$, respectively. In these coefficients, a quasi-particle is reflected from the spin channel \bar{s} into the spin channel \bar{s}' .

The wave function in ferromagnets for majority spin injection is represented by

$$\Psi_{\uparrow}(x) = e^{ik_F \bar{x}} \begin{pmatrix} 1 \\ 0 \\ 0 \\ 0 \end{pmatrix} + a_{\uparrow\uparrow} e^{ik_F \bar{x}} \begin{pmatrix} 0 \\ 0 \\ 1 \\ 0 \end{pmatrix} + a_{\uparrow\downarrow} e^{ik_F \bar{x}} \begin{pmatrix} 0 \\ 0 \\ 0 \\ 1 \end{pmatrix} \\ + b_{\uparrow\uparrow} e^{-ik_F \bar{x}} \begin{pmatrix} 1 \\ 0 \\ 0 \\ 0 \end{pmatrix} + b_{\uparrow\downarrow} e^{-ik_F \bar{x}} \begin{pmatrix} 0 \\ 1 \\ 0 \\ 0 \end{pmatrix}, \quad (18)$$

where $k_{F\downarrow} < k_S < k_{F\uparrow}$ and $k_S \approx \sqrt{2mE_F/\hbar^2}$. The wave function for minority spin injection is written in a similar way. The coefficients $a_{\bar{s}\bar{s}'}$ and $b_{\bar{s}\bar{s}'}$ are determined by solving the BdG equation with the quasiclassical approximation under appropriate boundary conditions.

The tunneling conductance $\sigma_T(eV)$ for finite temperature is given by⁶¹⁻⁶³

$$\sigma_T(eV) = \frac{2e^2}{h} G, \quad (19)$$

$$G = \frac{1}{16k_B T} \int_{-\infty}^{\infty} dE \int_{-\pi/2}^{\pi/2} d\theta_S \cos \theta_S [\sigma_{S\uparrow}(\theta_S) \\ + \sigma_{S\downarrow}(\theta_S)] \operatorname{sech}^2 \left(\frac{E - eV}{2k_B T} \right), \quad (20)$$

$$\sigma_{S\uparrow} = 1 + |a_{\uparrow\uparrow}|^2 - |b_{\uparrow\uparrow}|^2 \\ + \left(\frac{\eta_{\downarrow}}{\eta_{\uparrow}} |a_{\uparrow\downarrow}|^2 - \frac{\eta_{\downarrow}}{\eta_{\uparrow}} |b_{\uparrow\downarrow}|^2 \right) \Theta(\theta_C - |\theta_S|), \quad (21)$$

$$\sigma_{S\downarrow} = \left(1 + \frac{\eta_{\uparrow}}{\eta_{\downarrow}} |a_{\downarrow\uparrow}|^2 + |a_{\downarrow\downarrow}|^2 - \frac{\eta_{\uparrow}}{\eta_{\downarrow}} |b_{\downarrow\uparrow}|^2 - |b_{\downarrow\downarrow}|^2 \right) \\ \times \Theta(\theta_C - |\theta_S|), \quad (22)$$

with $Z_{\theta_S} = Z/\cos \theta_S$, $Z = 2mH/\hbar^2 k_F$, and $\eta_{\uparrow(\downarrow)} = \sqrt{1 \pm X/\cos^2 \theta_S}$. Here $X = U/E_F$ is defined as the spin-polarization parameter. The quantity $\sigma_{S\uparrow(\downarrow)}$ is the tunneling conductance for an incident electron with the majority (minority) spin. For $|\theta_S| > \theta_C = \cos^{-1} \sqrt{X}$, the reflected wave becomes an evanescent wave and does not contribute to the tunneling conductance. As shown in the above equations, the tunneling conductance depends on θ_M only when superconductors have spin-triplet Cooper pairs. The tunneling conductance can be summarized in simple equations in the following several cases. When θ_M is 0 or π in spin-triplet superconductors, the conductance is described by

$$\sigma_{S\uparrow} = \sigma_{N\uparrow}(A + B), \quad (23)$$

$$\sigma_{S\downarrow} = \sigma_{N\downarrow} C, \quad (24)$$

$$A = [1 - |\Gamma_+ \Gamma_-|^2 (1 - \sigma_{N\downarrow}) + \sigma_{N\downarrow} |\Gamma_+|^2] \Theta(\theta_C - |\theta_S|) / L_{D1}, \quad (25)$$

$$B = 1 - \Theta(\theta_C - |\theta_S|) [1 - |\Gamma_+ \Gamma_-|^2] / L_{D1}, \quad (26)$$

$$C = [1 - |\Gamma_+ \Gamma_-|^2 (1 - \sigma_{N\uparrow}) + \sigma_{N\uparrow} |\Gamma_+|^2] \Theta(\theta_C - |\theta_S|) / L_{D2}, \quad (27)$$

$$L_{D1} = |1 - \Gamma_+ \Gamma_- \sqrt{1 - \sigma_{N\downarrow}} \sqrt{1 - \sigma_{N\uparrow}} \exp[i(\varphi_{\downarrow} - \varphi_{\uparrow})]|^2, \quad (28)$$

$$L_{D2} = |1 - \Gamma_+ \Gamma_- \sqrt{1 - \sigma_{N\downarrow}} \sqrt{1 - \sigma_{N\uparrow}} \exp[i(\varphi_{\uparrow} - \varphi_{\downarrow})]|^2, \quad (29)$$

with

$$\exp(i\varphi_{\downarrow}) = \frac{1 - \eta_{\downarrow} + iZ_{\theta_S}}{\sqrt{1 - \sigma_{N\downarrow}}(1 + \eta_{\downarrow} - iZ_{\theta_S})}, \quad (30)$$

$$\exp(-i\varphi_{\uparrow}) = \frac{1 - \eta_{\uparrow} - iZ_{\theta_S}}{\sqrt{1 - \sigma_{N\uparrow}}(1 + \eta_{\uparrow} - iZ_{\theta_S})}. \quad (31)$$

The above equations can be applied to spin-singlet superconductors. When $\theta_M = \pi/2$ in spin-triplet superconductors, the conductance for each spin is given by

$$\sigma_{S\uparrow} = \sigma_{N\uparrow} \frac{1 - |\Gamma_+ \Gamma_-|^2 (1 - \sigma_{N\uparrow}) + \sigma_{N\uparrow} |\Gamma_+|^2}{|1 - \Gamma_+ \Gamma_- (1 - \sigma_{N\uparrow})|^2}, \quad (32)$$

$$\sigma_{S\downarrow} = \sigma_{N\downarrow} \frac{1 - |\Gamma_+ \Gamma_-|^2 (1 - \sigma_{N\downarrow}) + \sigma_{N\downarrow} |\Gamma_+|^2}{|1 - \Gamma_+ \Gamma_- (1 - \sigma_{N\downarrow})|^2} \Theta(\theta_C - |\theta_S|). \quad (33)$$

In the above equations, we define

$$\Gamma_{\pm} = \pm \frac{E - \sqrt{E^2 - |\Delta(\theta_S)|^2}}{\Delta(\theta_S)^*}, \quad (34)$$

$$\sigma_{N\uparrow} = \frac{4\eta_{\uparrow}}{(1 + \eta_{\uparrow})^2 + Z_{\theta_S}^2}, \quad (35)$$

$$\sigma_{N\downarrow} = \frac{4\eta_{\downarrow}}{(1 + \eta_{\downarrow})^2 + Z_{\theta_S}^2} \Theta(\theta_C - |\theta_S|). \quad (36)$$

In this paper, the dependence of the pair potential on temperatures is described by the BCS gap equation. The spatial dependence of the pair potential can be described by $\hat{\Delta}(\theta_S, x)$ with $\hat{\Delta}(\theta_S, x) = \check{\Delta}(\theta_S, x) \Theta(x)$. In order to determine the spatial dependence of $\check{\Delta}(\theta_S, x)$, we apply the quasiclassical Green's function theory developed by Hara and co-workers.^{2,58,64,65} In the following, we briefly explain the method in the case of spin-singlet superconductors. An extension to spin-triplet superconductors is straightforward.

The spatial dependence of $\check{\Delta}(\theta_S, x)$ is calculated by the diagonal elements of the matrix Green function $g_{\alpha\alpha}(x)$ which are represented by

$$g_{++}(\theta_S, x) = i \begin{pmatrix} \frac{1 + D_+(x)F_+(x)}{1 - D_+(x)F_+(x)} & \frac{2iF_+(x)}{1 - D_+(x)F_+(x)} \\ \frac{2iD_+(x)}{1 - D_+(x)F_+(x)} & -\frac{1 + D_+(x)F_+(x)}{1 - D_+(x)F_+(x)} \end{pmatrix}, \quad (37)$$

$$g_{--}(\theta_S, x) = i \begin{pmatrix} \frac{1 + D_-(x)F_-(x)}{-1 + D_-(x)F_-(x)} & \frac{2iF_-(x)}{-1 + D_-(x)F_-(x)} \\ \frac{2iD_-(x)}{-1 + D_-(x)F_-(x)} & -\frac{1 + D_-(x)F_-(x)}{-1 + D_-(x)F_-(x)} \end{pmatrix}, \quad (38)$$

where an index $\alpha = \pm$ specifies the direction of the momentum in the x direction. In these Green functions, $D_{\alpha}(x)$ and $F_{\alpha}(x)$ obey the following equations:

$$\begin{aligned} \hbar|v_{Fx}|D_{\alpha}(x) &= \alpha[2\omega_m D_{\alpha}(x) + \check{\Delta}(\theta_S, x)D_{\alpha}^2(x) \\ &\quad - \bar{\Delta}^*(\theta_S, x)], \end{aligned} \quad (39)$$

$$\begin{aligned} \hbar|v_{Fx}|F_{\alpha}(x) &= \alpha[-2\omega_m F_{\alpha}(x) + \bar{\Delta}^*(\theta_S, x)F_{\alpha}^2(x) \\ &\quad - \bar{\Delta}(\theta_S, x)], \end{aligned} \quad (40)$$

$$\check{\Delta}(\theta_S, x) = \begin{pmatrix} 0 & \bar{\Delta}(\theta_S, x) \\ -\bar{\Delta}(\theta_S, x) & 0 \end{pmatrix}. \quad (41)$$

The boundary conditions at the interface are given by^{66,67}

$$F_+(0) = \frac{(\eta_{\uparrow} - 1 + iZ)(\eta_{\downarrow} - 1 - iZ)}{(\eta_{\uparrow} + 1 + iZ)(\eta_{\downarrow} + 1 - iZ)} D_-(0)^{-1}, \quad (42)$$

$$F_-^{-1}(0) = \frac{(\eta_{\uparrow} - 1 + iZ)(\eta_{\downarrow} - 1 - iZ)}{(\eta_{\uparrow} + 1 + iZ)(\eta_{\downarrow} + 1 - iZ)} D_+(0). \quad (43)$$

We first solve $D_{\pm}(x)$ and $F_{\pm}(x)$ in Eqs. (39) and (40), then calculate $g_{\pm, \pm}(\theta, x)$ in Eqs. (37) and (38) for a given $\bar{\Delta}(\theta_S, x)$. By using $g_{\pm, \pm}(\theta, x)$, $\bar{\Delta}(\theta_S, x)$ is given by the following equations:

$$\check{\Delta}(\theta_S, x) = \sum_{n\alpha} \int_{\pi/2}^{\pi/2} d\theta_S' V(\theta_S, \theta_S') g_{\alpha, \alpha}(\theta_S', x), \quad (44)$$

$$V(\theta, \theta') = g_0 f(\theta) f(\theta'), \quad (45)$$

$$g_0 = \frac{2\pi k_B T}{\ln(T/T_C) + \sum_{0 < m < m_a} \frac{1}{m + 1/2}}, \quad (46)$$

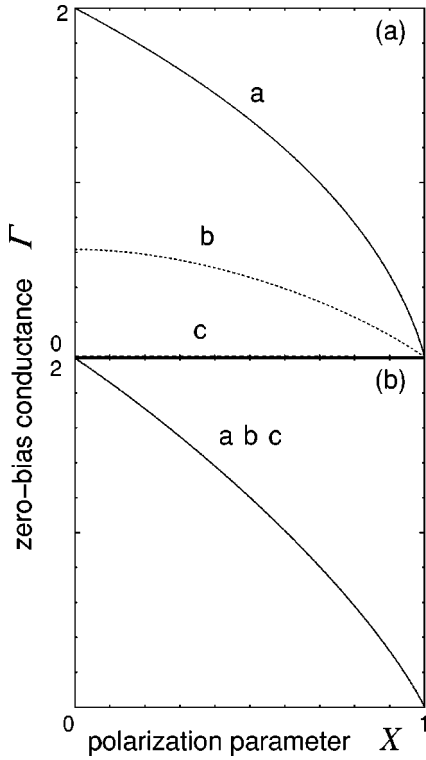


FIG. 2. X dependence of the zero-bias conductance Γ in non-SCF calculation for (a) $\alpha=0$ and (b) $\alpha=\pi/4$ in d -wave junctions at zero temperature. a: $Z=0$, b: $Z=1$, and c: $Z=5$.

where we introduce the cutoff m_a to regularize g_0 and $f(\theta)$ is given in Eqs. (10) and (16). The iteration is carried out until a sufficient convergence is obtained. In this way, we obtain $\bar{\Delta}(\theta, x)$, i.e., $\hat{\Delta}(\theta, x)$ self-consistently.

Under the pair potential in the self-consistent calculation, we obtain $\check{\Gamma}_{\pm}(x)$ by solving

$$i\hbar|v_{Fx}| \check{\Gamma}_{+}(x) = \alpha[2E\check{\Gamma}_{+}(x) - \bar{\Delta}(\theta_S, x)\check{\Gamma}_{+}^2(x) - \bar{\Delta}^*(\theta_S, x)], \quad (47)$$

$$i\hbar|v_{Fx}| \check{\Gamma}_{-}(x) = \alpha[2E\check{\Gamma}_{-}(x) - \bar{\Delta}^*(\theta_S, x)\check{\Gamma}_{-}^2(x) - \bar{\Delta}(\theta_S, x)]. \quad (48)$$

By replacing Γ_{\pm} in Eqs. (23)–(34) with $\check{\Gamma}_{\pm}(0)$, we can calculate the tunneling conductance. In what follows, we assume that the transition temperature of ferromagnets is much larger than T_C which is the transition temperature of superconductors. In such a situation, we can neglect the temperature dependence of X .

III. RESULTS

A. Polarization dependence of zero-bias conductance

In this subsection, we show the calculated results of the ZBC at zero temperature as a function of spin polarization in ferromagnets (X). The dimensionless ZBC (Γ) is given by

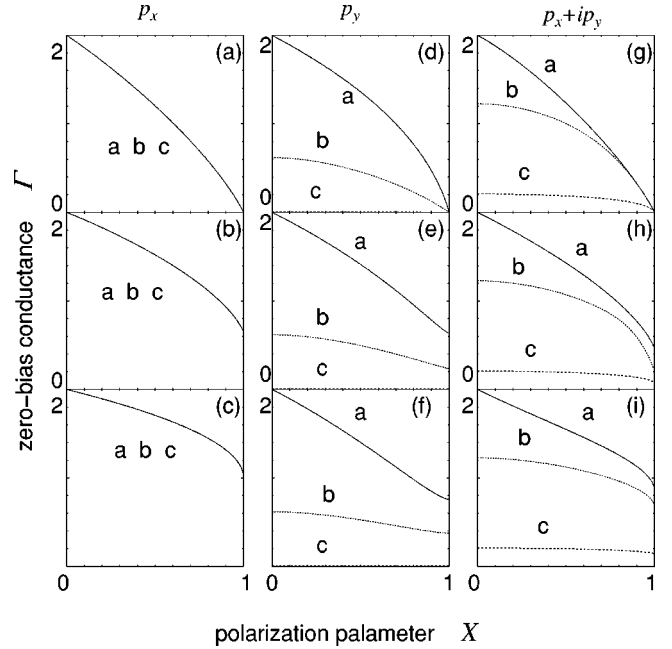


FIG. 3. X dependence of Γ in the non-SCF calculation. (a) $\theta_M=0$, (b) $\theta_M=\pi/4$, and (c) $\theta_M=\pi/2$ for p_x -wave junctions. (d) $\theta_M=0$, (e) $\theta_M=\pi/4$, and (f) $\theta_M=\pi/2$ for p_y -wave junctions. (g) $\theta_M=0$, (h) $\theta_M=\pi/4$, and (i) $\theta_M=\pi/2$ for p_x+ip_y -wave junctions. a: $Z=0$, b: $Z=1$ and c: $Z=5$.

$$\Gamma = \frac{\sigma_T(0)h}{2e^2}. \quad (49)$$

At first we show that the conductance obtained in the step-function model, where the spatial dependence of the pair potential is not determined self-consistently (non-SCF calculation). The X dependence of Γ at zero temperature for d -wave junctions is plotted in Fig. 2. The magnitude of Γ is always a decreasing function of X . For $\alpha=0$ [Fig. 2(a)], Γ decreases with increasing Z . On the other hand, for $\alpha=\pi/4$ [Fig. 2(b)], Γ is completely independent of Z because of the perfect Andreev reflection due to the zero-energy resonance state at the interface.

Secondly, we show the polarization dependence of Γ in triplet p_x -, p_y -, and p_x+ip_y -wave superconductor junctions as shown in Fig. 3, where the pair potentials are given in Eqs. (14), (15), and (16). The conductance depends on θ_M for all pairing symmetries. The spin degree of freedom remains in spin-triplet superconductors. As a consequence, the conductance depends on the relative angle between the magnetic moment in ferromagnets and the d vector in the superconductor. This is the characteristic feature of p -wave junctions. For $\theta_M=0$, as shown in Figs. 3(a), 3(d), and 3(g), Γ approaches zero in the limit of $X \rightarrow 1$ independent of Z . In these cases, the diagonal elements in Eq. (3) disappear and a quasiparticle suffers a spin flip in the Andreev reflection (i.e., $a_{\uparrow, \uparrow} = a_{\downarrow, \downarrow} = 0$). For $|\theta_S| > \theta_C$, the Andreev reflection to \uparrow spin becomes the evanescent wave. At the same time, an incident wave with \downarrow spin vanishes. Thus Γ vanishes in the limit of $X=1$, where ferromagnets are referred to as half

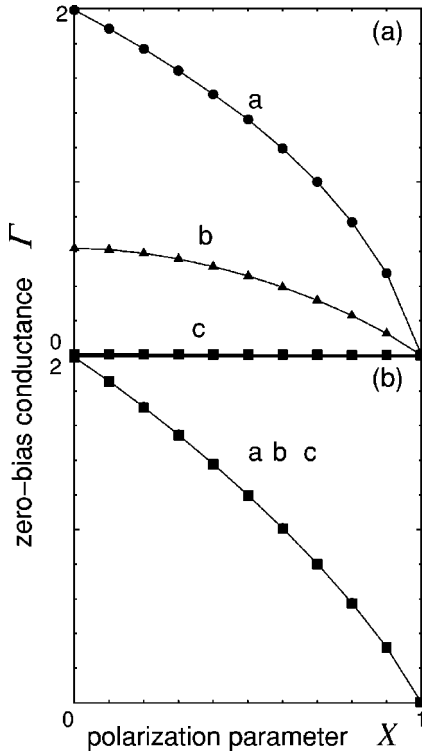


FIG. 4. X dependence of Γ in the SCF calculation for d -wave junctions. (a) $\alpha=0$ and (b) $\alpha=\pi/4$. a: $Z=0$, b: $Z=1$, and c: $Z=5$.

metals. On the other hand, for $\sin \theta_M \neq 0$, Γ takes finite values even in $X \rightarrow 1$ as shown in Figs. 3(b), 3(c), 3(e), 3(f), 3(h), and 3(i) because the spin-conserved Andreev reflection is still possible in these junctions. The results for $\theta_M = \pi/2$ are shown in Figs. 3(c), 3(f), and 3(i). In this case, the off-diagonal elements in Eq. (17) become zero. Thus, the spin of a quasiparticle is conserved in the Andreev reflection (i.e., $a_{\uparrow, \downarrow} = a_{\downarrow, \uparrow} = 0$). The Andreev reflection of an electron with \uparrow spin survives irrespective of θ_S , whereas that of an electron with \downarrow spin vanishes for $|\theta_S| > \theta_C$. We note that in p_x -wave junctions and d -wave junctions with $\alpha = \pi/4$, Γ does not depend on Z . This is because the ZES's are formed at the interface.

Thirdly we show the tunneling conductance under a pair potential whose spatial dependence is determined self-consistently (SCF calculation). The results for d -, p_x -, p_y -, and $p_x + ip_y$ -wave junctions are shown in Figs. 4 and 5. The conductance in the SCF calculation in Figs. 4 and 5 should be compared with corresponding results in the non-SCF calculation in Figs. 2 and 3, respectively. We do not find any remarkable differences between the results in the SCF calculation and those in the non-SCF calculation as shown in these figures.

Finally, the X dependence of Γ is plotted for various temperatures. As seen from Fig. 2(b), using tunneling through ZES, we can determine the magnitude of X using the value of Γ . This is a unique property for d -wave superconductors with $\alpha = \pi/4$ or p_x -wave junctions where all quasiparticles feel ZES independent of their directions of motions. Since Γ

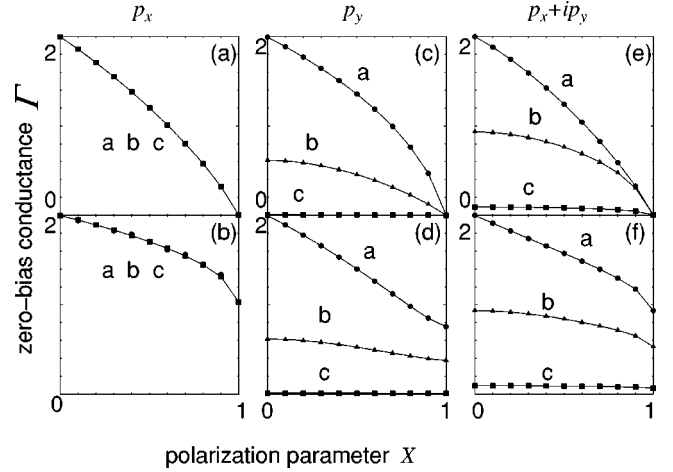


FIG. 5. X dependence of Γ in the SCF calculation. (a) $\theta_M=0$ and (b) $\theta_M=\pi/2$ with p_x -wave junctions. (c) $\theta_M=0$ and (d) $\theta_M=\pi/2$ with p_y -wave junctions. (e) $\theta_M=0$ and (f) $\theta_M=\pi/2$ with $p_x + ip_y$ -wave junctions. a: $Z=0$, b: $Z=1$, and c: $Z=5$.

is plotted at zero temperature in Fig. 2(b), it is actually important how this property holds even in finite temperatures. As shown in Fig. 6, when the magnitude of the temperature T is sufficiently smaller than T_C , Γ is almost insensitive to the magnitude of Z and we can estimate the magnitude of X through Γ . In the actual experiments, high- T_C cuprates, e.g., YBaCuO, BiSrCaCuO, with (110) oriented interfaces are promising candidates. In such a case, the actual value of $0.001T_C$ becomes 0.1 K and this temperature is fully accessible in the experiments.

B. Temperature dependence of zero-bias conductance

In this subsection, we discuss the temperature dependence of Γ . First, we show the conductance in the non-SCF calculation. Then the results are compared with those in the SCF calculation. Let us focus on d -wave junctions for $\alpha=0$ as shown in Figs. 7(a)–7(c), where the conductance is plotted as a function of temperature for several magnitudes of the exchange potential X . We note that in these junctions the ZES is not formed at the interface. For $Z=0$ [see Fig. 7(a)], the exchange potential in ferromagnets significantly affects the temperature dependence of Γ . For large X , Γ increases with the increase of T as shown in curve d in Fig. 7(a). The Andreev reflection (two-electron process) is suppressed by the large exchange potential and the current is mainly carried by a single electron process. While for small X , Γ decreases with the increase of T as shown in curve a in Fig. 7(a). This is because the current at zero voltage is mainly carried by two-electron processes through the Andreev reflection and the amplitude of the Andreev reflection is suppressed for $T \rightarrow T_C$. For $Z=5$ [Fig. 7(c)], Γ becomes small around $T \sim 0$ because the insulating barrier suppresses the Andreev reflection. The results show that Γ increases monotonically with increasing temperatures independent of X since the current is mainly carried by single electron process. For $Z=1$ [Fig. 7(b)], excepting for large X , the magnitude of Γ has a nonmonotonic temperature dependence, since the amplitude

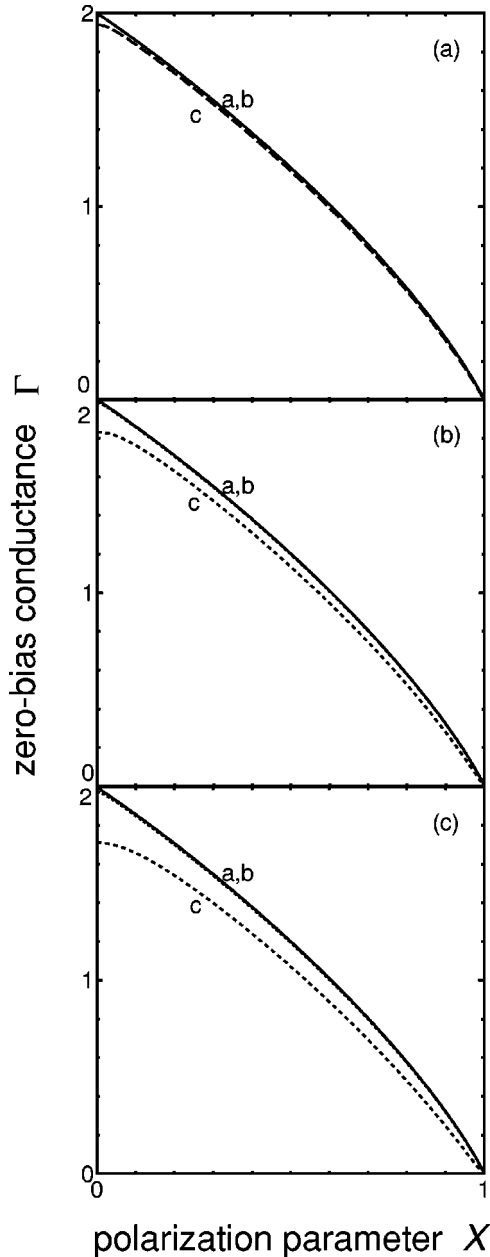


FIG. 6. X dependence of Γ for various temperatures for d -wave junctions for $\alpha = \pi/4$ in the non-SCF calculation. (a) $T/T_C = 0.001$, (b) $T/T_C = 0.005$, and (c) $T/T_C = 0.01$. a: $Z=0$, b: $Z=1$, and c: $Z=5$.

of single-electron processes (Andreev reflection) is enhanced (suppressed) with the increase of T .

Secondly we show the temperature dependence of Γ in d -wave junctions with $\alpha = \pi/4$ in Figs. 7(d)–7(f). For $Z = 0$, the line shape of the all curves in Fig. 7(d) are qualitatively similar to those with $\alpha = 0$ shown in Fig. 7(a) since ZES is not formed at the interface. We note that in Figs. 7(d)–7(f) Γ at zero temperature is independent of Z . The Andreev reflection is perfect in the limit of $Z = 0$. For finite Z , the ZES is formed at the interface which also leads to perfect Andreev reflection at $T = 0$. The characteristic behavior of the resonant tunneling can be seen in the conductance

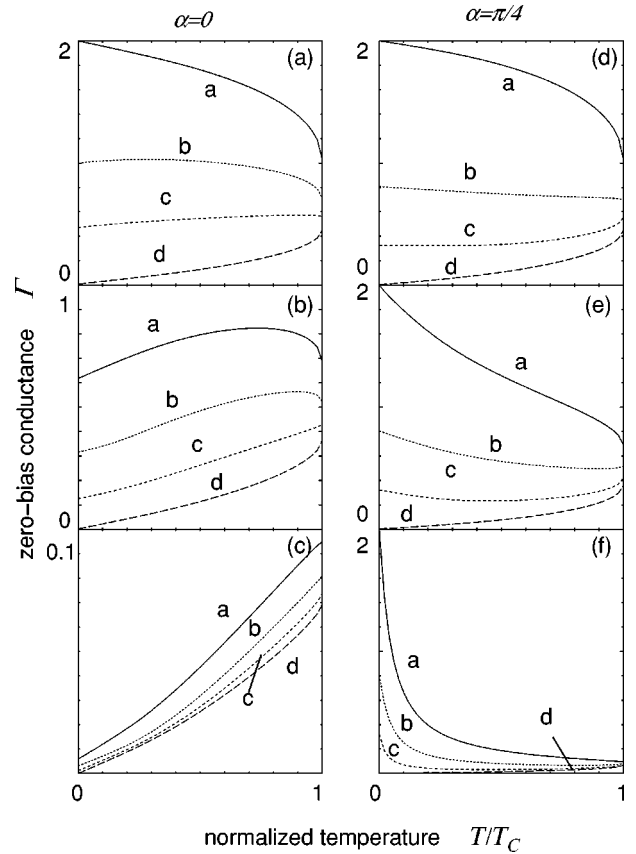


FIG. 7. Temperature dependence of Γ in the non-SCF calculation for d -wave junctions. (a) $Z=0$, (b) $Z=1$, and (c) $Z=5$ with $\alpha=0$. (d) $Z=0$, (e) $Z=1$, and (f) $Z=5$ with $\alpha = \pi/4$. a: $X=0$, b: $X=0.7$, c: $X=0.9$, and d: $X=0.999$.

for large Z . The amplitude of Γ is proportional to the inverse of T for intermediate temperatures [curve a in Fig. 7(f)]. Since the retroreflectivity of Andreev reflection is broken by exchange potentials, the degree of the resonance at the interface is weakened. As a result, the temperature dependence deviates from the inverse of T in curves b, c, and d in Fig. 7(f). For sufficiently large magnitudes of X , Γ becomes an increasing function of T for $T > 0.5T_C$ as shown in Fig. 7(f). In the case of a d wave with $\alpha = \pi/4$, we can estimate the magnitude of X from the temperature dependence of Γ .

Thirdly, we show temperature dependence of Γ in p_x -wave junctions with $\theta_M = 0$ in Figs. 8(a)–8(c) and those with $\pi/2$ in Figs. 9(a)–9(c). As shown in Figs. 8(a)–8(c), the temperature dependences of Γ are very similar to those of d -wave junctions with $\alpha = \pi/4$. When $\theta_M = 0$, Γ for small X is a decreasing function of T , whereas Γ for large X is an increasing function of T . In the case of $\theta_M = \pi/2$, however, Γ becomes a monotonic decreasing function of T independent of Z as shown in Figs. 9(a)–9(c). The spin of a quasiparticle is always conserved in the Andreev reflection in this case. Therefore the suppression of the conductance due to the breakdown of the retroreflectivity becomes weaker than that in the case of $\theta_M = 0$.

Next we show the conductance in p_y -wave junctions with $\theta_M = 0$ in Figs. 8(d)–8(f) and those with $\pi/2$ in Figs. 9(d)–9(f). In $\theta_M = 0$, the temperature dependence of Γ are similar

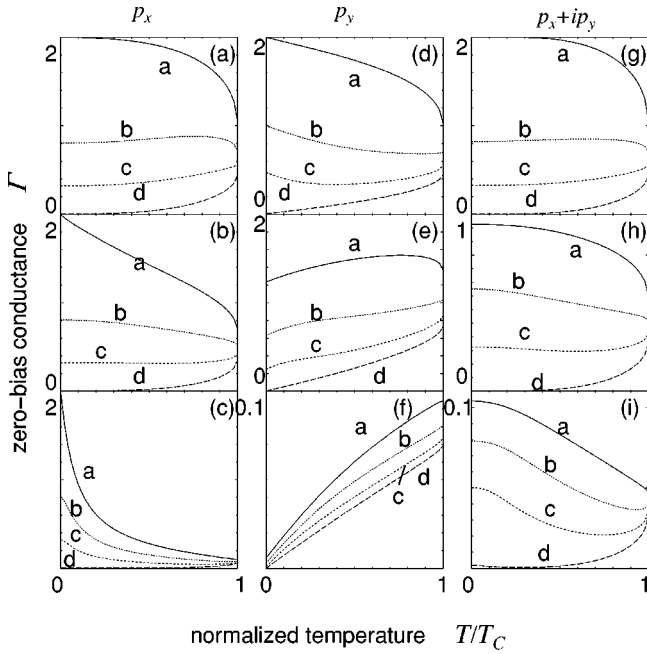


FIG. 8. Temperature dependence of Γ in the non-SCF calculation for $\theta_M=0$. (a) $Z=0$, (b) $Z=1$, and (c) $Z=5$ in p_x -wave junctions. (d) $Z=0$, (e) $Z=1$, and (f) $Z=5$ in p_y -wave junctions. (g) $Z=0$, (h) $Z=1$, and (i) $Z=5$ in p_x+ip_y -wave junctions. a: $X=0$, b: $X=0.7$, c: $X=0.9$, and d: $X=0.999$.

to those of d -wave junctions with $\alpha=0$ shown in Figs. 7(a)–7(c). In these junctions, no ZES is expected at the interface. In $\theta_M=\pi/2$ as shown in Figs. 9(d)–9(f), Γ for large X are larger than those with $\theta_M=0$ at low temperatures. In the case of $\theta_M=\pi/2$, the spin of a quasiparticle is conserved in the Andreev reflection, therefore, the suppression of conductance due to the breakdown of retroreflectivity becomes weaker than that in the case of $\theta_M=0$.

Finally we show the conductance in p_x+ip_y -wave junctions with $\theta_M=0$ in Figs. 8(g)–8(i) and those with $\pi/2$ in Figs. 9(g)–9(i). In p_x+ip_y -wave junctions with $\theta_M=0$, the temperature dependence of Γ can be understood by a combination of the results in p_x - and p_y -wave junctions because the ZES is only expected for a quasiparticle incident perpendicular to the interface.³² As seen from Fig. 8(g) for $Z=0$, there is no clear difference between Γ in p_x+ip_y -wave junctions with $\theta_M=0$ and corresponding results in the p_x - or p_y -wave junctions shown in Figs. 8(a) and 8(d). For a finite barrier potential at $Z=1$, the line shape of all the curves in Fig. 8(h) is more similar to the corresponding results in the p_x -wave junctions than those in the p_y -wave junctions. However, the Γ 's are smaller than those in the p_x -wave junctions. For $Z=5$, Γ for small X are enhanced at low temperatures because of the ZES [see curve a in Fig. 8(i)]. On the other hand, for large X , Γ is an increasing function of T [see curve d in Fig. 8(i)]. For $\theta_M=\pi/2$, Γ becomes a decreasing function of T for all cases as shown in Figs. 9(g)–9(i). These features are similar to those in the p_x -wave junctions.

It is important to check how the above results are modified in the presence of the spatial dependence in the pair potential near the interface. We show the conductance in the

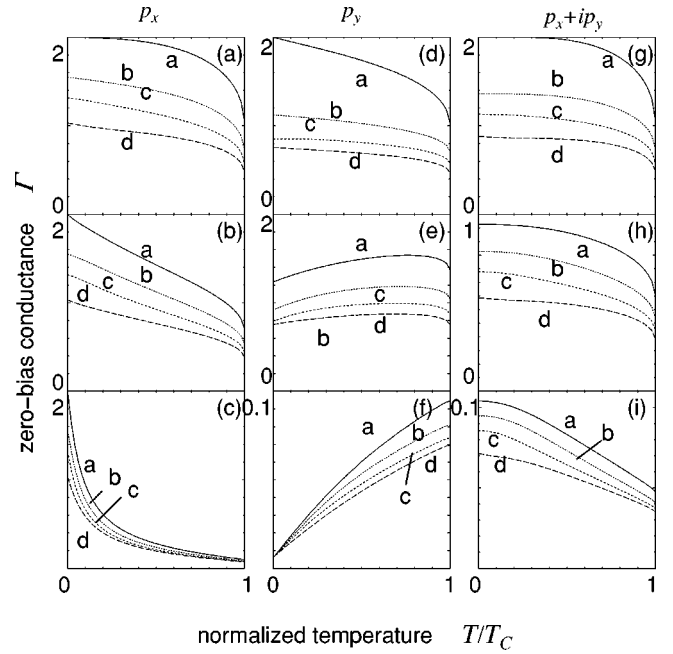


FIG. 9. Temperature dependence of Γ in the non-SCF calculation for $\theta_M=\pi/2$. (a) $Z=0$, (b) $Z=1$, and (c) $Z=5$ in p_x -wave junctions. (d) $Z=0$, (e) $Z=1$, and (f) $Z=5$ in p_y -wave junctions. (g) $Z=0$, (h) $Z=1$, and (i) $Z=5$ in p_x+ip_y -wave junctions. a: $X=0$, b: $X=0.7$, c: $X=0.9$, and d: $X=0.999$.

SCF calculation in the second part of this subsection. In what follows, we consider two cases of X , $X=0$ (curve a) and $X=0.9$ (curve b). The corresponding results in the non-SCF calculation are curves a ($X=0$) and c ($X=0.9$) from Figs. 7–9.

In Fig. 10, we show the conductance in the SCF calculation in the d -wave junctions with $\alpha=0$ and $\pi/4$. It is found that the temperature dependences of Γ with $\alpha=0$ in the SCF calculation are very similar to those in the non-SCF calculation when we compare the results in Figs. 7(a)–7(c) with those in Figs. 10(a)–10(c). The same tendency can be seen between the results of d -wave junctions with $\alpha=\pi/4$ in Figs. 7(d)–7(f) and those in Figs. 10(d)–10(f). When ZES's are formed at the interface, the profile of the pair potential significantly deviates from the step function. The characteristic behavior of the conductance in the SCF, however, is qualitatively the same as those in the non-SCF. From the calculated results, we conclude that the conductance is insensitive to the profile of the pair potential. This is because the resonant tunneling through the ZES dominates the conductance. We note that the ZES is a consequence of the sign change of the pair potential.

In p_x -wave junctions, line shapes of Γ for $\theta_M=0$ shown in Figs. 11(a)–11(c) are very similar to those in d -wave junctions with $\alpha=\pi/4$. For $\theta_M=\pi/2$, as shown in Figs. 12(a)–12(c), the magnitudes of Γ are slightly larger than those in Figs. 11(a)–11(c). These features are similar to those found in the non-SCF calculation in Figs. 8(a)–8(c) and Figs. 9(a)–9(c). As well as in the p_x -wave junctions, the characteristic behavior of Γ in SCF results in p_y -wave junctions shown in Figs. 11(d)–11(f) and Figs. 12(d)–12(f) are almost the same

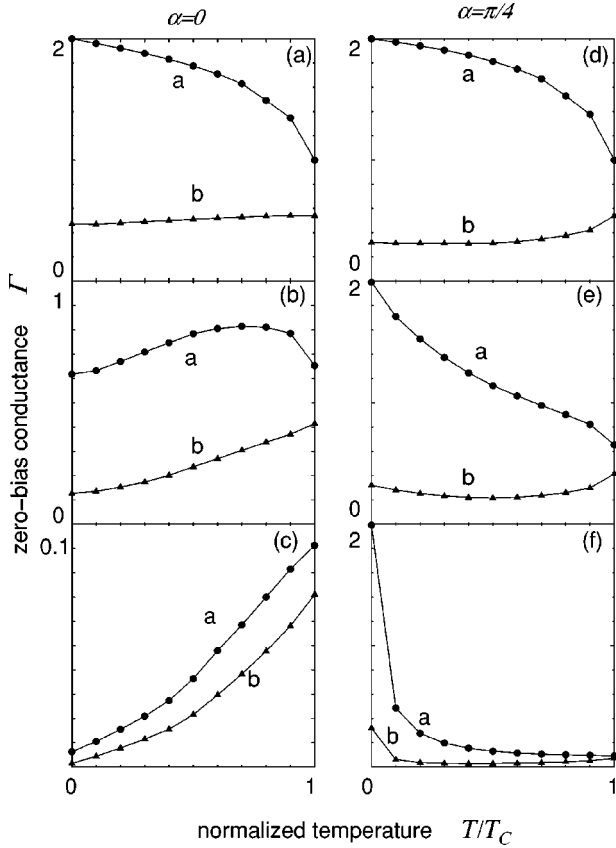


FIG. 10. Temperature dependence of Γ in the SCF calculation for d -wave junctions. (a) $Z=0$, (b) $Z=1$, and (c) $Z=5$ with $\alpha=0$. (d) $Z=0$, (e) $Z=1$, and (f) $Z=5$ for $\alpha=\pi/4$. a: $X=0$ and b: $X=0.9$.

with those obtained in the non-SCF calculation shown in Figs. 8(d)–8(f) and Figs. 9(d)–9(f).

In the case of $p_x + ip_y$ -wave symmetry, the line shapes of Γ for (g) and (h) in Figs. 11 and 12 are similar to those in the non-SCF results shown in (g) and (h) in Figs. 8 and 9. However, the temperature dependences of Γ based on the SCF calculation deviate from those in the non-SCF one for large Z [Figs. 11(i) and 12(i)]. In the SCF calculation, Γ first decreases with the increase of T then increases. The decreasing part is similar to that in the p_x -wave case and is explained by the ZES. The increasing part is similar to that in the p_y -wave junctions. Since only a quasiparticle injected perpendicular to the interface contributes to the ZES, the effects of the spatial dependence of the pair potentials on the conductance are not negligible.²⁸

IV. SUMMARY

In this paper, we have calculated the polarization and temperature dependence of the zero-bias conductance (ZBC) in $F/I/S$ junctions, where we have chosen d -wave symmetry of the pair potential for high- T_C cuprates and $p_x + ip_y$ wave for Sr₂RuO₄. As a reference, we have also studied the conductance in p_x - and p_y -wave junctions. We have established a formalism of the ZBC which is available for arbitrary θ_M

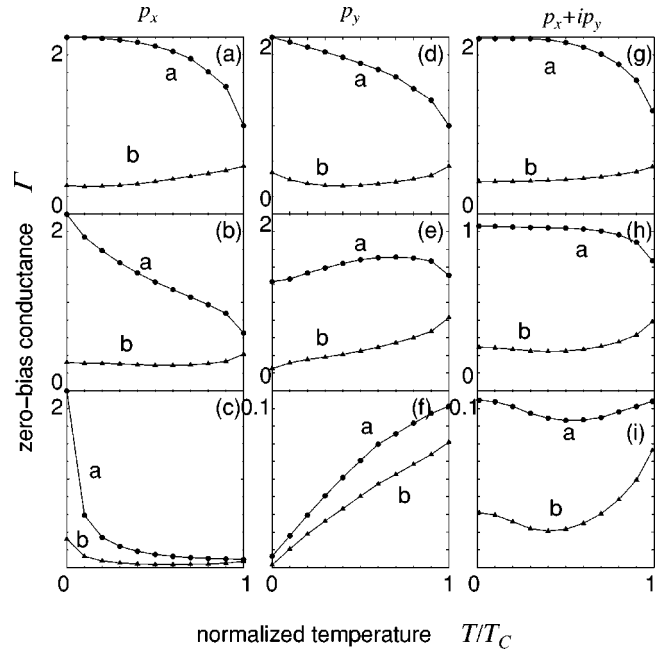


FIG. 11. Temperature dependence of Γ in the SCF calculation for $\theta_M=0$. (a) $Z=0$, (b) $Z=1$, and (c) $Z=5$ in p_x -wave junctions. (d) $Z=0$, (e) $Z=1$, and (f) $Z=5$ in p_y -wave junctions. (g) $Z=0$, (h) $Z=1$, and (i) $Z=5$ in $p_x + ip_y$ -wave junctions. a: $X=0$ and b: $X=0.9$.

which is the angle between the magnetization axis in ferromagnet and c axis of superconductors. The θ_M dependence of the tunneling conductance only appears in the spin-triplet superconductor junctions. On the basis of the numerical re-

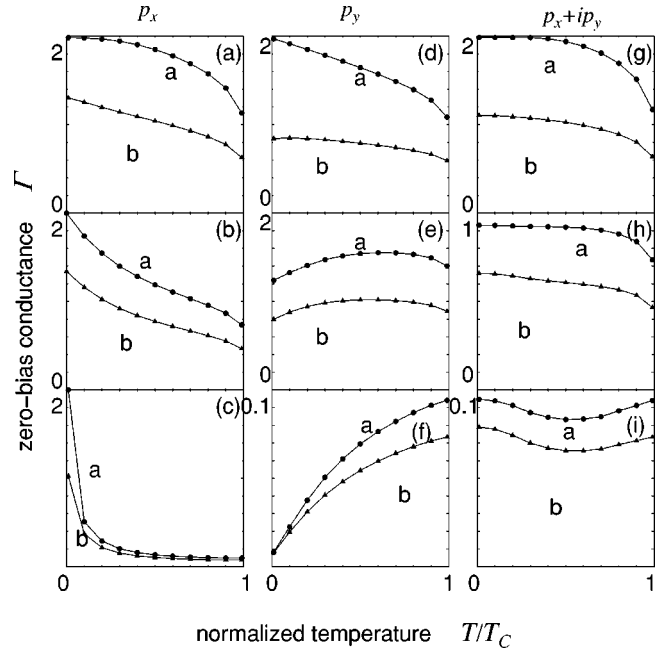


FIG. 12. Temperature dependence of Γ in the non-SCF calculation for $\theta_M=\pi/2$. (a) $Z=0$, (b) $Z=1$, and (c) $Z=5$ in p_x -wave junctions. (d) $Z=0$, (e) $Z=1$, and (f) $Z=5$ in p_y -wave junctions. (g) $Z=0$, (h) $Z=1$, and (i) $Z=5$ in $p_x + ip_y$ -wave junctions. a: $X=0$ and b: $X=0.9$.

sults, we reach the following conclusions.

(1) When injected quasiparticles from ferromagnets always feel the zero-energy resonance state, e.g., d -wave junctions with (110) orientation and p_x -wave junctions, the zero-bias tunneling conductance (ZBC) at zero temperature is insensitive to the barrier potential at the interface. This property is useful for the determination of the degree of spin polarization in ferromagnets at sufficiently low temperatures. One of the promising candidates is LaSrMnO/YBaCuO(BiSrCaCuO) with a well oriented (110) interface. Within our theory, below 0.1 K we can estimate the magnitude of the polarization of ferromagnets through the value of the conductance of the junctions.

(2) For d -wave junctions with (110) orientation and p_x -wave junctions, the ZBC decreases with increasing temperatures when the degree of the polarization X is small. For large X , the ZBC is an increasing function of T . The presence of the ZES explains these behaviors. In d -wave junctions with (100) orientation and p_y -wave junctions, the ZBC is an increasing function of T independent of X . This is because the ZES does not appear at these junction interfaces. For $p_x + ip_y$ -wave junctions, the ZBC first decreases with increasing T then increases.

(3) In p -wave junctions, the temperature dependence of the ZBC depends on the direction of the magnetization axis of ferromagnets because of the spin degree of freedom of Cooper pairs in spin-triplet superconductors.

(4) Throughout this paper, we have calculated the ZBC in two ways. (i) The spatial dependence of the pair potential is assumed to be a step function (non-SCF calculation), (ii) the spatial depletion of the pair potentials is determined self-consistently (SCF calculation). We have confirmed that there are no remarkable differences between the conductance in the non-SCF calculation and those in the SCF calculation.

In this paper, effects of random potentials in ferromagnets are not taken into account. Recently, there have been several works on random scattering effects in unconventional superconductor junctions.^{68–72} It is actually interesting to study transport properties of junctions where diffusive ferromagnets are attached to unconventional superconductors. In the present paper, the splitting of the ZBCP by magnetic fields through the Zeeman effect or magnetic impurities in an insulator are not taken into account.^{40–42} These are interesting and important future issues.

ACKNOWLEDGMENTS

This work was partially supported by the Core Research for Evolutional Science and Technology (CREST) of the Japan Science and Technology Corporation (JST). J.I. acknowledges support by the NEDO international Joint Research project “Nano-scale Magnetoelectronics.”

-
- ¹L.J. Buchholtz and G. Zwirgagl, Phys. Rev. B **23**, 5788 (1981).
²J. Hara and K. Nagai, Prog. Theor. Phys. **76**, 1237 (1986).
³C.R. Hu, Phys. Rev. Lett. **72**, 1526 (1994).
⁴S. Kashiwaya, Y. Tanaka, M. Koyanagi, H. Takashima, and K. Kajimura, Phys. Rev. B **51**, 1350 (1995).
⁵L. Alff, H. Takashima, S. Kashiwaya, N. Terada, H. Ihara, Y. Tanaka, M. Koyanagi, and K. Kajimura, Phys. Rev. B **55**, 14 757 (1997).
⁶M. Covington, M. Aprili, E. Paraoanu, L.H. Greene, F. Xu, J. Zhu, and C.A. Mirkin, Phys. Rev. Lett. **79**, 277 (1997).
⁷J.Y.T. Wei, N.-C. Yeh, D.F. Garrigus, and M. Strasik, Phys. Rev. Lett. **81**, 2542 (1998).
⁸W. Wang, M. Yamazaki, K. Lee, and I. Iguchi, Phys. Rev. B **60**, 4272 (1999).
⁹I. Iguchi, W. Wang, M. Yamazaki, Y. Tanaka, and S. Kashiwaya, Phys. Rev. B **62**, R6131 (2000).
¹⁰Y. Tanaka and S. Kashiwaya, Phys. Rev. B **53**, 9371 (1996).
¹¹Y. Tanaka and S. Kashiwaya, Phys. Rev. B **53**, 11 957 (1996); **56**, 892 (1997); **58**, 2948 (1998).
¹²Y. Tanaka and S. Kashiwaya, J. Phys. Soc. Jpn. **68**, 3485 (1999); **69**, 1152 (2000).
¹³Y. Asano, Phys. Rev. B **63**, 052512 (2001); **64**, 014511 (2001); J. Phys. Soc. Jpn. **71**, 905 (2002).
¹⁴Y. Tanuma, Y. Tanaka, M. Yamashiro, and S. Kashiwaya, Phys. Rev. B **57**, 7997 (1998).
¹⁵Y. Tanuma, Y. Tanaka, M. Ogata, and S. Kashiwaya, J. Phys. Soc. Jpn. **67**, 1118 (1998).
¹⁶Y. Tanuma, Y. Tanaka, M. Ogata, and S. Kashiwaya, Phys. Rev. B **60**, 9817 (1999).
¹⁷Y. Tanaka, T. Asai, N. Yoshida, J. Inoue, and S. Kashiwaya, Phys. Rev. B **61**, R11 902 (2000).
¹⁸Y. Tanaka, Y. Tanuma, and S. Kashiwaya, Phys. Rev. B **64**, 054510 (2001).
¹⁹Y. Tanaka, H. Tsuchiura, Y. Tanuma, and S. Kashiwaya, J. Phys. Soc. Jpn. **71**, 271 (2002).
²⁰Y. Tanaka, H. Itoh, H. Tsuchiura, Y. Tanuma, J. Inoue, and S. Kashiwaya, J. Phys. Soc. Jpn. **71**, 2005 (2002).
²¹S. Ryu and Y. Hatsugai, Phys. Rev. Lett. **89**, 077002 (2002).
²²Y. Tanaka and S. Kashiwaya, Phys. Rev. Lett. **74**, 3451 (1995).
²³S. Kashiwaya, Y. Tanaka, M. Koyanagi, and K. Kajimura, Phys. Rev. B **53**, 2667 (1996).
²⁴S. Kashiwaya and Y. Tanaka, Rep. Prog. Phys. **63**, 1641 (2000).
²⁵T. Löfwander, V.S. Shumeiko, and G. Wendin, Semicond. Sci. Technol. **14**, R53 (2001).
²⁶M. Yamashiro, Y. Tanaka, and S. Kashiwaya, Phys. Rev. B **56**, 7847 (1997).
²⁷M. Yamashiro, Y. Tanaka, Y. Tanuma, and S. Kashiwaya, J. Phys. Soc. Jpn. **67**, 3224 (1998).
²⁸M. Yamashiro, Y. Tanaka, N. Yoshida, and S. Kashiwaya, J. Phys. Soc. Jpn. **68**, 2019 (1999).
²⁹C. Honerkamp and M. Sigrist, J. Low Temp. Phys. **111**, 898 (1998); Prog. Theor. Phys. **100**, 53 (1998).
³⁰Y. Asano, Phys. Rev. B **64**, 224515 (2001).
³¹Y. Tanaka, Y. Tanuma, K. Kuroki, and S. Kashiwaya, J. Phys. Soc. Jpn. **71**, 2102 (2002).

- ³²Y. Tanaka, T. Hirai, K. Kusakabe, and S. Kashiwaya, *Phys. Rev. B* **60**, 6308 (1999).
- ³³F. Laube, G. Goll, H.v. Löhneysen, M. Fogelström, and F. Lichtenberg, *Phys. Rev. Lett.* **84**, 1595 (2000).
- ³⁴Z.Q. Mao, K.D. Nelson, R. Jin, Y. Liu, and Y. Maeno, *Phys. Rev. Lett.* **87**, 037003 (2001).
- ³⁵C. Wälti, H.R. Ott, Z. Fisk, and J.L. Smith, *Phys. Rev. Lett.* **85**, 5258 (2000).
- ³⁶K. Sengupta, I. Žutić, H.-J. Kwon, V.M. Yakovenko, and S. Das Sarma, *Phys. Rev. B* **63**, 144531 (2001).
- ³⁷Y. Tanuma, K. Kuroki, Y. Tanaka, and S. Kashiwaya, *Phys. Rev. B* **64**, 214510 (2001).
- ³⁸Y. Tanuma, K. Kuroki, Y. Tanaka, R. Arita, S. Kashiwaya, and H. Aoki, *Phys. Rev. B* **66**, 094507 (2002).
- ³⁹A.F. Andreev, *Zh. Éksp. Teor. Fiz.* **46**, 1823 (1964) [*Sov. Phys. JETP* **19**, 1228 (1964)].
- ⁴⁰J.X. Zhu, B. Friedman, and C.S. Ting, *Phys. Rev. B* **59**, 9558 (1999).
- ⁴¹S. Kashiwaya, Y. Tanaka, N. Yoshida, and M.R. Beasley, *Phys. Rev. B* **60**, 3572 (1999).
- ⁴²I. Zutic and O.T. Valls, *Phys. Rev. B* **60**, 6320 (1999); **61**, 1555 (2000).
- ⁴³N. Yoshida, Y. Tanaka, J. Inoue, and S. Kashiwaya, *J. Phys. Soc. Jpn.* **68**, 1071 (1999).
- ⁴⁴N. Stefanakis, *Phys. Rev. B* **64**, 224502 (2001); *J. Phys.: Condens. Matter* **13**, 3643 (2001).
- ⁴⁵T. Hirai, N. Yoshida, Y. Tanaka, J. Inoue, and S. Kashiwaya, *J. Phys. Soc. Jpn.* **70**, 1885 (2001).
- ⁴⁶T. Hirai, N. Yoshida, Y. Tanaka, J. Inoue, and S. Kashiwaya, *Physica C* **367**, 137 (2002).
- ⁴⁷A. Buzdin, *Phys. Rev. B* **62**, 11 377 (2000).
- ⁴⁸G.Y. Sun, D.Y. Xing, J.M. Dong, and M. Liu, *Phys. Rev. B* **65**, 174508 (2002).
- ⁴⁹Z.C. Dong, D.Y. Xing, and J. Dong, *Phys. Rev. B* **65**, 214512 (2002).
- ⁵⁰N. Yoshida, H. Itoh, H. Tsuchiura, Y. Tanaka, J. Inoue, and S. Kashiwaya, *Physica C* **367**, 185 (2002).
- ⁵¹N. Yoshida, H. Itoh, T. Hirai, Y. Tanaka, J. Inoue, and S. Kashiwaya, *Physica C* **367**, 165 (2002).
- ⁵²Z.Y. Chen, A. Biswas, I. Zutic, T. Wu, S.B. Ogale, R.L. Greene, and T. Venkatesan, *Phys. Rev. B* **63**, 212508 (2001).
- ⁵³A. Sawa, S. Kashiwaya, H. Obara, H. Yamasaki, M. Koyanagi, Y. Tanaka, and N. Yoshida, *Physica C* **339**, 107 (2000).
- ⁵⁴H. Kashiwaya, A. Sawa, S. Kashiwaya, H. Yamazaki, M. Koyanagi, I. Kurosawa, Y. Tanaka, and I. Iguchi, *Physica C* **357-360**, 1610 (2001).
- ⁵⁵C.-C. Fu, Z. Huang, and N.-C. Yeh, *Phys. Rev. B* **65**, 224516 (2002).
- ⁵⁶Y. Nagato and K. Nagai, *Phys. Rev. B* **51**, 16 254 (1995).
- ⁵⁷M. Matsumoto and H. Shiba, *J. Phys. Soc. Jpn.* **64**, 3384 (1995); **64**, 4867 (1995); **65**, 2194 (1995).
- ⁵⁸Y. Ohashi, *J. Phys. Soc. Jpn.* **65**, 823 (1996).
- ⁵⁹A. Millis, D. Rainer, and J.A. Sauls, *Phys. Rev. B* **38**, 4504 (1988).
- ⁶⁰C. Bruder, *Phys. Rev. B* **41**, 4017 (1990).
- ⁶¹G.E. Blonder, M. Tinkham, and T.M. Klapwijk, *Phys. Rev. B* **25**, 4515 (1982).
- ⁶²A.V. Zaitsev, *Zh. Éksp. Teor. Fiz.* **86**, 1742 (1984) [*Sov. Phys. JETP* **59**, 1015 (1984)].
- ⁶³A.L. Shelankov, *J. Low Temp. Phys.* **60**, 29 (1985).
- ⁶⁴M. Ashida, S. Aoyama, J. Hara, and K. Nagai, *Phys. Rev. B* **40**, 8673 (1989).
- ⁶⁵Y. Nagato, K. Nagai, and J. Hara, *J. Low Temp. Phys.* **93**, 33 (1993).
- ⁶⁶T. Hirai, Y. Tanaka, and J. Inoue (unpublished).
- ⁶⁷Y. Tanuma, Y. Tanaka, and S. Kashiwaya, *Phys. Rev. B* **64**, 214519 (2001).
- ⁶⁸H. Itoh, Y. Tanaka, J. Inoue, and S. Kashiwaya, *Physica C* **367**, 99 (2002).
- ⁶⁹Y. Asano and Y. Tanaka, *Phys. Rev. B* **65**, 064522 (2002).
- ⁷⁰Y. Tanaka, Y. Nazarov, and S. Kashiwaya, *Phys. Rev. Lett.* (to be published).
- ⁷¹N. Yoshida, Y. Asano, H. Itoh, Y. Tanaka, J. Inoue, and S. Kashiwaya, *J. Phys. Soc. Jpn.* **72**, 895 (2003).
- ⁷²The present model deals with the ideal situation where the height of the ZBCP is only a function of the polarization of the ferromagnet. However, in real junctions, the interface quality and the impurity distribution near the interface may have influences on the ZBCP height. Detailed analysis of such factors will be discussed in future papers.